

## ROOM-TEMPERATURE MULTI-FERROCITY IN OFF-STOICHIOMETRIC $\text{Bi}_{1.1}\text{FeO}_3$ CERAMICS PREPARED BY MELT-PHASE SINTERING

\*M. S. AWAN and A. S. BHATTI

Center for Micro and Nano Devices, Department of Physics, COMSATS Institute of Information Technology,  
Park Road, Islamabad, Pakistan

(Received May 13, 2009 and accepted in revised form October 06, 2009)

---

Off-stoichiometric multiferroic ( $\text{Bi}_{1.1}\text{FeO}_3$ ) ceramics were synthesized by the conventional powder metallurgy route by adopting the melt-phase sintering followed by rapid thermal quenching technique. Samples were sintered at four different temperatures (775-850) °C/120min in air. It was observed that high temperature sintering is desirable in order to avoid the impurity phases. Perovskite and impurity phases were identified by X-ray diffraction (XRD) analysis performed at room temperature. Ferroelectric properties were measured by plotting the P-E loops under an applied field of 80 KV/cm. Sample sintered at 850°C showed spontaneous polarization, remnant polarization, and coercive field of 14.44  $\mu\text{C}/\text{cm}^2$ , 5.47  $\mu\text{C}/\text{cm}^2$  and 25.50 kV/cm, respectively. The linear behavior of magnetization as a function of applied magnetic field confirms the antiferromagnetic nature of the  $\text{BiFeO}_3$  compound at room temperature. Scanning electron microscopic (SEM) studies revealed the dense and submicron features of the sintered samples. It is suggested that causes leading to the higher leakage currents and dielectric break down can be suppressed by adopting the melt-phase sintering followed by rapid thermal quenching technique. This technique was also found effective in increasing the density of the ceramic samples. The sintering technique developed in this work is expected to be useful in synthesizing other ceramics from multivalent or volatile starting materials.

**Keywords:** Multiferroic oxides, Perovskite,  $\text{BiFeO}_3$ , Melt-phase sintering, Spontaneous polarization, Polarization hysteresis, Dielectric break

---

### I. Introduction

Multiferroics are the class of materials having coupled ferroelectric and ferro/antiferromagnetic order parameters that result in simultaneous ferroelectricity and magnetism in the single phase [1]. These materials, therefore, not only have potential applications in magnetic and ferroelectric devices, but also the ability to couple the electric and the magnetic polarization in these materials, providing an additional degree of freedom in device design [2-6]. This class of materials would offer a large application potential for new devices taking advantage of two coupled degrees of freedom based on local off-centered distortion and electron spin. The major applications of multiferroic materials are in spintronic devices, functional sensors and multi-state memory devices [3-6]. Fundamental physics of these materials is also very interesting and fascinating besides the practical applications. The choice of such materials is very much limited due to inherent lack of

simultaneous ferroelectric and ferromagnetic orders in a single phase at room temperature.

The main multiferroic perovskite oxides studied so far include  $\text{Bi}_{1.1}\text{FeO}_3$ ,  $\text{BiMnO}_3$  and  $\text{ReMnO}_3$  (Re = Y, Ho-Lu). Among them, BFO bearing high Curie temperature ( $T_C \sim 830^\circ\text{C}$ ) and a high Néel temperature ( $T_N \sim 370^\circ\text{C}$ ) is technologically more desirable [7-8]. BFO has a rhombohedrally distorted perovskite crystal structure with space group R3c and G-type anti-ferromagnetism at room temperature [9]. The ferroelectric mechanism in BFO is conditioned by the stereochemically active  $6s^2$  lone pair of ( $\text{Bi}^{3+}$ ) while the weak magnetic property is caused by residual moment from the canted ( $\text{Fe}^{3+}$ ) spin structure [10]. The magneto-electric (ME) coupling effect between magnetic and electric behaviours occur through the lattice distortion of BFO when an electric field or a magnetic field is applied [6], which opened new avenues to the device design and application.

---

\* Corresponding author : sss\_awan@yahoo.com

Though  $\text{BiFeO}_3$  was discovered in the early 1960's and its structure and properties have been extensively studied [11-12] transport measurements have been hampered by leakage problems. Low resistivity of the sample at room temperature makes the observation of the ferroelectric loop very difficult. This seriously limited the application of this material. In order to enhance the resistivity and observe a hysteresis loop, measurements were done at 80 K by Teague et al. [13]. They obtained a ferroelectric hysteresis loop from a single crystal, with a spontaneous polarization of  $3.5 \mu\text{C}/\text{cm}^2$  in the (100) direction, but the saturation of the loop was not observed even at fields as high as 55 kV/cm. Latter, Wang and Pradhan [14-15] adopted the rapid thermal sintering technique (RTST) and claimed the saturated ferroelectric loop at room temperature. They observed that spontaneous polarization, remnant polarization, and the coercive field were  $8.9 \mu\text{C}/\text{cm}^2$ ,  $4.0 \mu\text{C}/\text{cm}^2$ , and 39 kV/cm respectively; under an applied field of 100 kV/cm. They sintered the ceramic sample at 880 °C for 400 and 450 sec. It was proposed that very high heating rate and short sintering time is beneficial for suppressing the leakage currents and to make it possible the measurement of ferroelectric loop at room temperature. Observation of saturated ferroelectric hysteresis loops in  $\text{BiFeO}_3$  thin films at room temperature has been reported [7, 16]. There are several reports [17-18] on the fabrication of BFO dispersed in  $\text{BaTiO}_3$  matrix to restrict the second phase, leakage current and low resistivity in the sample. This enables the study of physical properties of  $\text{BiFeO}_3$  rich phases. Other research work on  $\text{BiFeO}_3$  ceramic involved synthesizing pure phase  $\text{BiFeO}_3$  by leaching the impurity phase with dilute nitric acid [19] but the saturated loop was not obtained in this pure phase  $\text{BiFeO}_3$  ceramic due to its lower density and high conductivity. For the investigation of electric properties and practical applications of  $\text{BiFeO}_3$  ceramics, it is necessary and still a growing challenge to synthesize phase-pure and resistive samples. Liquid-phase sintering followed by rapid thermal quenching technique is improved processing technique used for the fabrication of BFO ceramics. However, detailed studies on microscopic grains, thermal, magnetic, and electrical properties related to frequency dependent dielectric loss are still lacking in this potentially important ceramic.

In this paper, we report the synthesis and characterization of off-stoichiometric ( $\text{Bi}_{1.1}\text{FeO}_3$ ) ceramic samples by adopting the melt-phase sintering and rapid thermal quenching technique. SEM micrographs reveal the dense and submicron features of the sintered samples. Pinched and loose ferroelectric loops have been observed at room temperature in these ceramic samples. Linear behavior of magnetization as a function of applied magnetic field reveals the antiferromagnetic nature of the  $\text{BiFeO}_3$  ceramic. This technique may be applied to other perovskite oxide materials.

## 2. Experiment

Ceramic samples of off-stoichiometric multiferroic  $\text{Bi}_{1.1}\text{FeO}_3$  were prepared by the conventional powder metallurgy route adopting the melt-phase sintering followed by rapid thermal quenching technique. High purity  $\text{Bi}_2\text{O}_3$  (99.99%) and  $\text{Fe}_2\text{O}_3$  (99.99%) powders were weighed in off-stoichiometric proportions (Bi:Fe = 1.1:1 mole ratio). Wet mixing technique was applied to achieve the homogeneous mixture of the starting materials. Acetone was used as the wetting medium. After thorough washing of the ball mill jar, raw powders, acetone and ceramic balls were put into the ball mill and milling was carried out for five hours. The powder to ball ratio was 1:10. After mixing the slurry was drawn into the petty dish and let it to dry in the fume hood over night. The next day, flake like dried powder was ground and mixed with the help of motor and pestle for more than two hours. Mixed powder was then calcined at 725 °C for 60 minutes in air. After calcinations the powder was again ground for two hours in order to remove agglomerates formed during calcinations. Then 3% PVA was added as the binding agent. The role of binder is to strengthen the green body and to keep contact among the powder particles. The binder added mixture was then uni-axially pressed (5 MPa) into the disk like green compact with diameter ( $\phi = 15\text{mm}$ ) and thickness ( $T = 5\text{mm}$ ). Then the prepared disk like pellets were sintered by following the heat treatment cycle given in Figure 1. Sintering temperature was optimized for which samples were sintered at four different temperatures i.e. 775, 800, 825 and 850 °C. The sintering cycle includes five steps. In the first step green compact was heated slowly from room temperature (RT) to 400 °C at the rate of 1 °C/min. The heating rate was kept very slow in order to

remove the binder safely without cracking the pellet. In the second step sample was kept at this temperature (400 °C) for 60 minutes for complete removal of the binder. In the third step temperature was raised to 850 °C at a rate of 4 °C/min. In the fourth isothermal step temperature was kept at 850 °C for 120 minutes. In this step sintering of the green compact took place. Finally the sample was air quenched by removing it from the heated furnace quickly. The idea was that melt-phase sintering followed by quenching may restrict the secondary phases in the sintered sample. This may help to improve the electrical properties as secondary phases may cause leakage currents. Actually, there may not be sufficient time during quenching for impurity/second phases to be stable.

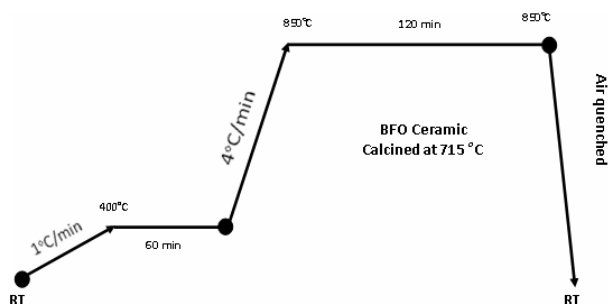


Figure 1. Heat treatment cycle for sintering of  $\text{BiFeO}_3$  ceramic samples.

For electrical measurements the samples were prepared to have a clean and smooth surface for electrodes. With the help of diamond cutter pellets were cut into slices of thickness  $\sim 4\text{-}5$  mm. Later these slices were further thinned down to 1.5 mm thickness by grinding on the silicon carbide sand paper. Finally samples were polished with the help of diamond paste and then dried with the compressed air to remove the contamination. These neat and clean surfaces were used for electrode connections for electrical measurements. Silver (Ag) paste electrodes with a 1.5 mm diameter were pasted on both sides of the samples. Ferroelectric properties of the synthesized  $\text{BiFeO}_3$  ceramics were measured using a RT6000 ferroelectric tester under virtual ground conditions. All measurements were carried out at room temperature.

### 3. Results and Discussion

Figure 2 presents the x-ray diffraction (XRD) patterns of the  $\text{BiFeO}_3$  ceramic samples prepared

by melt-phase sintering and rapid thermal quenching techniques. Samples were characterized for XRD studies between the  $2\theta$ -scan regions of ( $20^\circ - 60^\circ$ ). BFO samples were sintered at four different temperatures i.e 775, 800, 825, and 850 °C. All the samples were sintered for 120 minutes and then air quenched. The phase analysis was performed by considering the hexagonal BFO unit cell. The hexagonal unit cell of BFO system contains two formula pseudocubic.

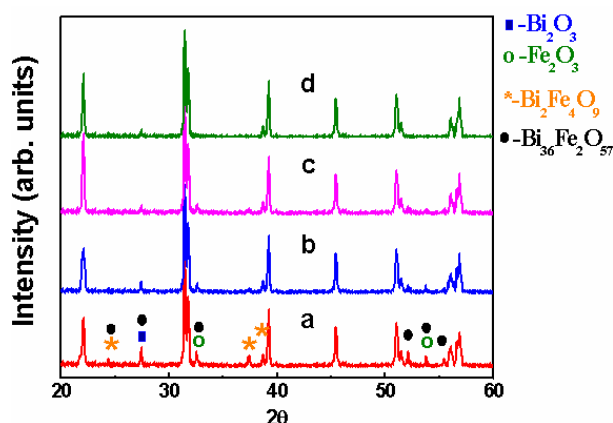


Figure 2. XRD patterns of the  $\text{BiFeO}_3$  ceramic samples sintered at (a) 775°C (b) 800°C (c) 825°C and (d) 850°C. All the samples were sintered for 120 minutes in air and air quenched.

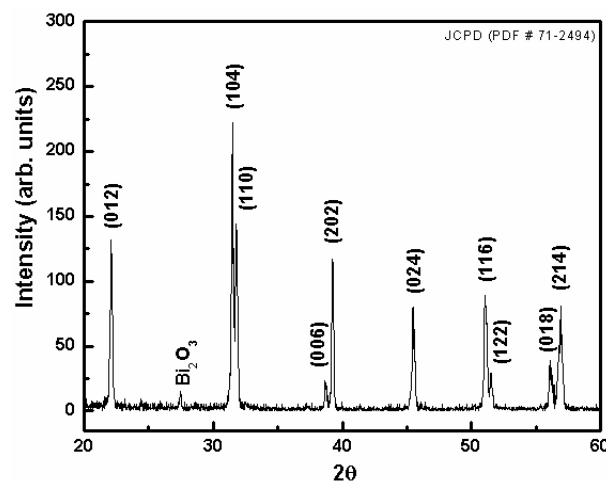


Figure 3. Indexed X-ray diffraction (XRD) pattern of the  $\text{BiFeO}_3$  ceramic sample sintered at 850°C for 120 minutes in air, where index (hkl) is based on the hexagonal crystal structure (JCPD card-PDF # 71-2494).

units (distorted cubic) cells of  $\text{BiFeO}_3$ . The lattice parameters for hexagonal unit cell of  $\text{BiFeO}_3$  were calculated by using the XRD software named

“CELL”. The indexed XRD pattern for BFO is shown in Figure 3. The (hkl) planes in the XRD pattern for BFO were indexed by comparing them with the data of JCPD card of PDF # 71-2494. Using  $2\theta$ -values from the XRD graph and (hkl) values from the standard JCPD card the lattice parameters for the hexagonal unit cell were generated. The calculated values are given as  $a = 5.58(1) \text{ \AA}$  and  $c = 13.87(4) \text{ \AA}$ . The reported lattice parameters for the BFO hexagonal unit cell are  $a = 5.58(1) \text{ \AA}$  and  $c = 13.86(2) \text{ \AA}$ . The calculated values of the lattice parameters for the hexagonal unit cell of  $\text{BiFeO}_3$  matched well with the values reported in the literature. The major reflection was from the (110) peak which appeared at ( $2\theta = 31.49^\circ$ ). All other BFO peaks were marked and identified by comparison. For low temperature sintering ( $775^\circ\text{C}$ ) some additional peaks appeared in the XRD graph like at ( $2\theta = 27.43^\circ$  and  $32.61^\circ$ ) are the reflections from unreacted  $\text{Bi}_2\text{O}_3$  and  $\text{Fe}_2\text{O}_3$  powders respectively. Some non-perovskite impurity phases like  $\text{Bi}_2\text{Fe}_4\text{O}_9$  and  $\text{Bi}_{36}\text{Fe}_2\text{O}_{57}$  were also identified. The presence of these unreacted powders and impurity phases may be attributed to the use of unsuitable sintering temperature. One other reason may be that  $\text{Bi}_2\text{O}_3$  is not fully liquefied under these sintering conditions as its melting point is ( $\sim 817^\circ\text{C}$ ). In other parts of the samples, the remaining liquefied  $\text{Bi}_2\text{O}_3$  may be insufficient to form  $\text{BiFeO}_3$  phase, resulting in unreacted powders ( $\text{Bi}_2\text{O}_3$ ,  $\text{Fe}_2\text{O}_3$ ) and impurity phases as shown in Figure 2(a). We kept the sintering time constant and vary the sintering temperature. Later the samples prepared under the identical conditions were sintered at 800, 825 and  $850^\circ\text{C}$  for 120 minutes. On increasing the sintering temperature the peaks due to unreacted powders ( $\text{Bi}_2\text{O}_3$  and  $\text{Fe}_2\text{O}_3$ ) were reduced and also other impurity-phases were eliminated to some extent as shown in Figure-2(b-d). The XRD pattern in Figure 2(d) can be indexed only for perovskite BFO phase. It is believed that at sintering temperature the low melting point ( $\text{Bi}_2\text{O}_3$ ) powder converts into the liquid phase. This ( $\text{Bi}_2\text{O}_3$ ) liquid wet the ( $\text{Fe}_2\text{O}_3$ ) powder particles. As a result, ( $\text{Bi}_2\text{O}_3$ ) react with ( $\text{Fe}_2\text{O}_3$ ) powder particles to form the desired ( $\text{BiFeO}_3$ ) phase. We obtained phase-pure BFO ceramic sample with a little additional peak from ( $\text{Bi}_2\text{O}_3$ ) for the sintering temperature of  $850^\circ\text{C}$  as shown in Figure 2(d). This additional peak may be due to the use of excess ( $\text{Bi}_2\text{O}_3$ ) powder in the starting material. Similar kind of behavior is also observed by some other researchers [14, 20-21].

The impurity phases appeared in the sample prepared by melt-phase sintering and rapid thermal quenching techniques at  $825^\circ\text{C}$  may be attributed to the fact that this sintering temperature is very close to the melting point of the  $\text{Bi}_2\text{O}_3$  ( $\sim 817^\circ\text{C}$ ). During sintering at ( $825^\circ\text{C}$ ) the melting of  $\text{Bi}_2\text{O}_3$  was probably not complete. Therefore the liquid  $\text{Bi}_2\text{O}_3$  is insufficient to wet the whole  $\text{Fe}_2\text{O}_3$  particles and it is not possible to complete the solid-state reaction between the powders. As a result we observed some additional peaks along with the main  $\text{BiFeO}_3$  peaks. This can be seen in Figure-2(c). As the mixture powder was calcined prior to sintering, XRD patterns in Figure 4 give the phase development in the sintered and calcined material. For comparison the XRD pattern of the powder mixture of well mixed raw materials is also presented in Figure 4(a). After calcination the powder is not completely converted into  $\text{BiFeO}_3$  phase. It is noted that the sintering temperature less than  $850^\circ\text{C}$  is not sufficient for sintering of BFO samples. Sintering at lower temperatures resulted in the formation of undesirable phases which ultimately affected the ferroelectric properties.

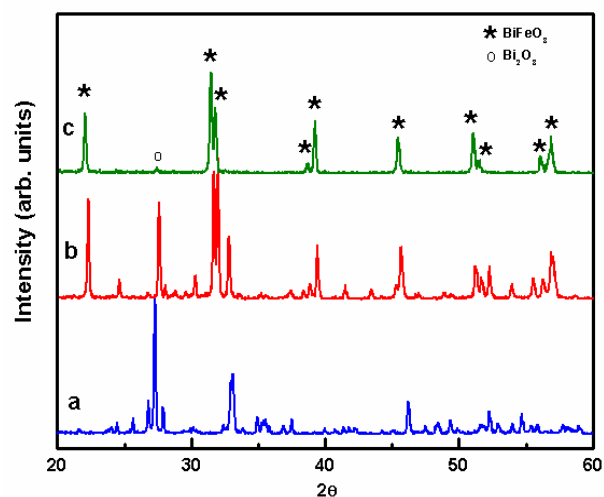


Figure 4. XRD patterns of the (a) powder mixture of  $\text{Bi}_2\text{O}_3$  and  $\text{Fe}_2\text{O}_3$  (b) powder calcined at  $725^\circ\text{C}$  for 60 minutes (c)  $\text{BiFeO}_3$  ceramic sample sintered at  $850^\circ\text{C}$  for 120 minutes in air.

Figure 5 shows the magnetization of the BFO ceramic sample as a function of applied magnetic field. The measurement was carried out on the ceramic sample sintered at  $850^\circ\text{C}$  for 120 minutes at room temperature. It is evident that magnetization is a linear function of applied

magnetic field. This behaviour is typical of antiferromagnetic materials [22]. On the other hand, the magnetization and magnetic hysteresis results confirm the absence of canted ferromagnetic behavior in this sample. This suggests the absence of Fe-related clusters or impurities in the sample. Surface morphology of the sintered ceramic samples was investigated by the SEM studies. Figure 6 is the SEM micrographs of the samples sintered at 775°C and 850°C for 120 minutes, respectively. SEM pictures were taken after thermal etching of the ceramic samples. For thermal etching the sintered sample was exposed in the furnace at 800 °C for short interval of time (10 minutes). As a result of this we can observe the etched features of the sintered sample. It is evident from the SEM micrographs that they consist of mixed cores and fine particles. The microstructure of the sample sintered at 850°C is relatively dense. Small and big particles are well connected to each other. Less porosity, smooth surface and impurity free well connected grains are essential for the good ferroelectric properties.

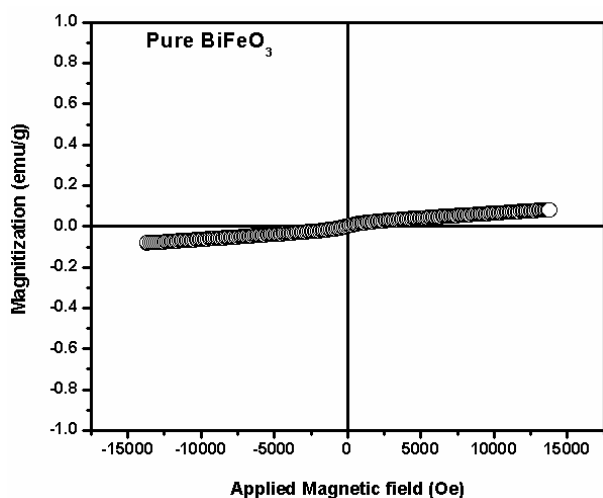
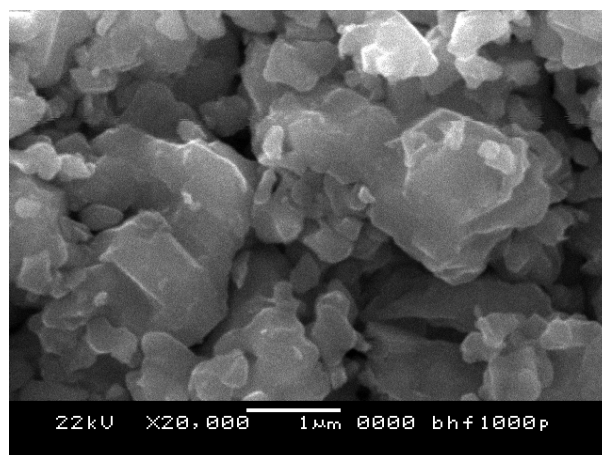


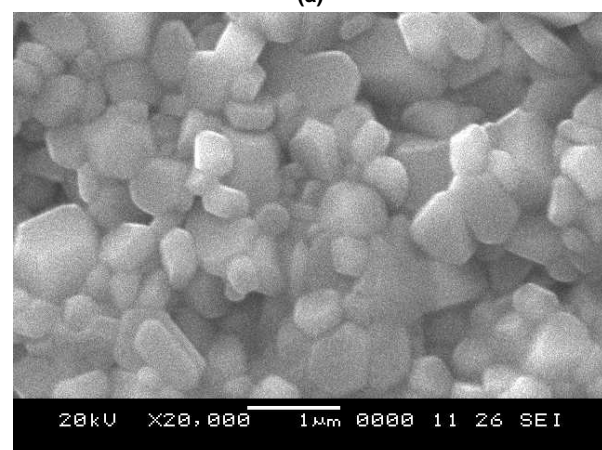
Figure 5. Magnetization behaviour of BiFeO<sub>3</sub> ceramic sample (sintered at 850°C) as a function of applied magnetic field.

During sintering limited diffusion of the particles can take place and as a result necking between the particles is formed as shown by SEM micrograph in Figure 6(b). The empty space between the particles is reduced and hence bulk density of the ceramic sample improves. Furthermore, the existence of liquid-phase during the sintering process will also be beneficial to increase the bulk density of the sintered ceramic

samples. During sintering process increase in the bulk density was observed. Figure 7 is the graph between the relative bulk densities of the sintered BiFeO<sub>3</sub> ceramic samples at different temperatures. The density was measured by Archimedes method. The graph shows a rapid increase in the bulk density during sintering between the temperatures (800-825) °C. The density increases from 53% to 74% when the sintering temperature is increased from 800 °C to 825 °C. It should be noted that this change in apparent bulk density is just across the melting point of Bi<sub>2</sub>O<sub>3</sub>, which is ~817 °C. A relative density of 81% was observed when the samples were sintered at 850 °C, indicating that compact ceramic could be synthesized using this technique. Porosity and density significantly affects the ferroelectric properties.



(a)



(b)

Figure 6. SEM micrographs of the BiFeO<sub>3</sub> ceramic sample sintered at (a) 775°C for 120 minutes (b) 850°C for 120 minutes. Picture reveals submicron features and was taken after thermal etching.

Ferroelectric properties were conducted by measuring polarization (P-E) hysteresis loops of the ceramic samples. Figure 8 is the P-E loops of the BFO samples sintered at 775 and 850 °C. The measurements were carried out for an applied field of 80 KV/cm. Sample sintered at 775 °C showed a pinched P-E loop with very low ferroelectric properties. This may be due to the porous microstructure and/or presence of impurity/secondary phases as indicated by the XRD results. Sample sintered at 850 °C was phase pure and showed a slim and loose P-E loop with the spontaneous polarization, remnant polarization, and coercive field are 14.44  $\mu\text{C}/\text{cm}^2$ , 5.47  $\mu\text{C}/\text{cm}^2$  and 25.50 kV/cm, respectively. These results are in agreement with the results obtained by others [23]. It is known that the deviation from oxygen stoichiometry (non-perovskite phases) leads to valence fluctuation of Fe ions from (+3 to +2 state) in  $\text{BiFeO}_3$ , resulting in high conductivity [24]. Our explanation for the resistive off-stoichiometric  $\text{BiFeO}_3$  ceramic samples synthesized by the melt-phase sintering and rapid thermal quenching technique is that excess  $\text{Bi}_2\text{O}_3$  will cover the Bi loss caused due to its evaporation. This will maintain the required stoichiometry of the BFO compound. On the other hand rapid thermal quenching may reduce the formation of undesired phases.

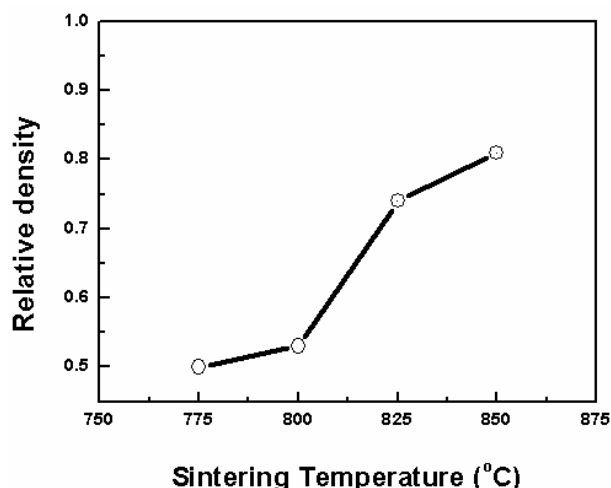


Figure 7. Relative bulk density of  $\text{BiFeO}_3$  ceramics sintered at different temperatures

#### 4. Conclusion

In conclusion, a phase-pure  $\text{BiFeO}_3$  ceramic was synthesized using a Melt-phase sintering and rapid thermal quenching techniques. Pinched and

slim polarization hysteresis loops were observed at room temperature. Sintering temperature improved the bulk density upto 81%. SEM micrographs revealed submicron particles with dense microstructure developed after sintering at 850 °C for 120 minutes in air. Magnetic measurements confirmed that ceramic  $\text{BiFeO}_3$  is antiferromagnetic at room temperature. The BFO materials synthesized in this work provide a possibility for further study of electric properties and the practical applications of  $\text{BiFeO}_3$  ceramic. The sintering technique developed in this work will also be useful in synthesizing other materials from volatile or multivalent components. In future we will use these ceramic samples as target material for the fabrication of multiferroic thin films on various substrates by pulsed laser deposition (PLD) and sputtering techniques.

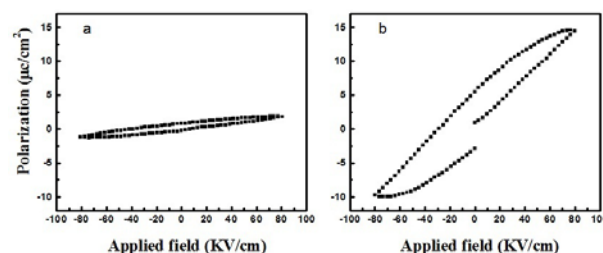


Figure 8. Polarization (P-E) hysteresis loops of  $\text{BiFeO}_3$  ceramics sintered at (a) 775°C (b) 850°C.

#### References

- [1] J. F. Scott. *Nat. Mater* **6** (2007) 256.
- [2] W. Eerenstein, N. D. Mathur and J. F. Scott: *Nature* **442** (2006) 759.
- [3] M. Li, *J. Phys. D: Appl. Phys.* **40** (2007) 160377.
- [4] S. Dong, J-F. Li and D. Viehland: *Appl. Phys. Lett.* **83** (2003) 2265.
- [5] S. Dong: *Appl. Phys. Lett.* **89** (2006) 243512.
- [6] S.W Cheong and M. Mostovoy: *Nature Mater.* **6** (2007) 13.
- [7] J. Wang, J. B. Neaton, H. Zheng, V. Nagarajan, S. B. Ogale, B. Liu, D. Viehland, V. Vaithyanathan, D. G. Schlom, U. V. Waghmare, N. A. Spaldin, K. M. Rabe, M. Wuttig, and R. Ramesh: *Science* **299** (2003) 1719.

- [8] J. B. Neaton, C. Ederer, U. V. Waghmare, N. A. Spaldin and K. M. Rabe: *Phys. Rev.* **71** (2005) 14 13.
- [9] G. A. Smolenskii and I. E. Chupis, *Sov. Phys.Usp.* **25** (1982) 475.
- [10] P. Fischer: *J. Phys. C: Solid State Phys.* **13** (1980) 1931.
- [11] J. D. Bucci, B. K. Robertson and W. J. James: *J. Appl. Crystallogr.* **5** (1972) 178.
- [12] F. Kubel and H. Schmid: *Acta Crystallogr., Sect. B: Struct. Sci.* **46** (1990) 698.
- [13] J. R. Teague, R. Gerson, and W. J. James, *Solid State Commun.* **8** (1970) 1073.
- [14] Y. P. Wang, L. Zhou, M. F. Zhang, X. Y. Chen, J.-M. Liu and Z. G. Liua: *Appl. Phys. Lett.* **84** (2004) 1731.
- [15] A. K. Pradhan, Kai Zhang, D. Hunter, J. B. Dadson, G. B. Loutts, P. Bhattacharya, R. Katiyar, Jun Zhang, D. J. Sellmyer, U. N. Roy, Y. Cui, and A. Burger: *J. Appl. Phys.* **97** (2005) 093903.
- [16] V. R. Palkar, J. John and R. Pinto: *Appl. Phys. Lett.* **80** (2002) 1628.
- [17] K. Ueda, H. Tabata and T. Kawai, *Appl. Phys. Lett.* **75** (1999) 555.
- [18] M. M. Kumar, A. Srinivas, and S. V. Suryanarayan, *J. Appl. Phys.* **87** (2000) 855
- [19] M. M. Kumar, V. R. Palkar, K. Srinivas and S. V. Suryanarayana: *Appl. Phys. Lett.* **76** (2000) 2764.
- [20] C. Tabares-Munoz, J. P. Rivera, A. Monnier and H. Schmid: *Jpn. J. Appl. Phys.* **24** (1985) 1051.
- [21] I. Sosnowska, T. Peterlin-Neumaier and E. Steichele: *J. Phys. C* **15** (1982) 4835.
- [22] V. R. Palkar, Darshan C. Kundaliya, S. K. Malik and S. Bhattacharya: *Phy. Rev.* **B 69**, (2004) 212102.
- [23] Shan-Tao Zhang, Ling-Hua Pang, Yi Zhang, Ming-Hui Lu, and Yan-Feng Chen: *J. Appl. Phys.* **100** (2006) 114108.
- [24] V. R. Palkar, J. John and R. Pinto, *Appl. Phys. Lett.* **80** (2002) 1628.